

Mathematical Modelling of Bifacial Photovoltaic-Thermal (BPVT) Collector with Mirror Reflector

Muslizainun Mustapha*, Ahmad Fudholi*[‡], Kamaruzzaman Sopian*

*Solar Energy Research Institute, National University of Malaysia, Malaysia

(muslizainun@gmail.com, a.fudholi@ukm.edu.my, ksopian@ukm.edu.my)

[‡] Corresponding Author; Ahmad Fudholi, Solar Energy Research Institute, National University of Malaysia

Tel: +06 8911 8479, a.fudholi@ukm.edu.my

Received: 03.02.2020 Accepted: 10.04.2020

Abstract- Hybrid photovoltaic-thermal (PVT) collectors were developing to produce both electrical and thermal energy simultaneously. Energy production of PVT collectors can be improved with employment of a bifacial photovoltaic (PV) panel. Bifacial PV panel has potential to capture sunlight from both front and back surfaces to generate more electrical energy. This study presents a bifacial PVT (BPVT) collector integrated with v-groove mirror reflector by using air as a cooling fluid. The v-groove mirror reflector design was implemented to enhance absorption of sunlight from the lower face of the bifacial panel. Air flows through the channels to remove excessive heat from the panel in order to raise panel efficiency. The aim of this paper is to develop a mathematical modeling for energy analysis of BPVT collector and solved using matrix inversion method. The mathematical models were studied at steady-state condition and based on the first and second laws of thermodynamics. The combined effects of solar radiation, mass flow rate and packing factor of bifacial PV panel on the energy efficiency of the BPVT collector were investigated. The results obtained show that at solar radiation of 863Wm^{-2} the BPVT has the highest energy efficiency value of 57% for 0.66 of packing factor, at mass flow rate of $0.02\text{-}0.08\text{kg/s}$. In addition, PVT collector with bifacial PV panel has efficiency value of 70% is greater than PVT collector with monofacial PV panel, which has efficiency of 50% under the same operating conditions.

Keywords Bifacial, photovoltaic-thermal, efficiency, electrical energy, thermal energy.

1. Introduction

Solar energy can be considered an eco-friendly energy production [1] and photovoltaic (PV) technology is one of the most popular solar energy technologies and is widely adopted in industry and housing [2], [3]. PV cells convert solar radiation into electricity and it has about 20% of electrical conversion efficiency [4]. Increasing temperature of the PV cells by 1°C caused a decrease in PV cells efficiency of 0.5% for the crystalline silicon PV cells and approximately 0.25% for the amorphous silicon PV cells [5]. Several researchers have suggested to use cooling fluids such as air and water to remove excessive heat from the PV cells in order to control PV cells' temperature [6]–[8]. This approach, known as the hybrid PVT solar collector, can produce both thermal and electrical energy at the same time.

In the last years, numerous experimental and theoretical studies on the energy performances of PVT collector have

been conducted [9]–[11]. These studies demonstrate that hybrid PVT collector can generate more energy per unit area than two separate units [12]. Salem et. al [13] conducted an experiment of PVT collector using aluminium cooling plate with straight and helical channels. The study indicated that the energy efficiency varied from 59.3% to 80.4% at the mass flow rate 0.25 to 1.0 L/min. Yet another research, Fudholi et. al [14] examined the performances analysis of PVT air collector with ∇ -groove absorber. The total electrical energy obtained was 10% and thermal efficiency was about 83% at air flow rate of 0.007kg/s to 0.07kg/s.

According to the existing literature, most of the PVT collector was constructed by using monofacial PV panel [15]. There are limited studies done on experimental and theoretical of PVT collector integrated with bifacial PV panel. Bifacial PV panel is having two active surfaces to absorb sunlight, in contrast with monofacial PV where the upper side is transparent with glazing to capture sunlight and back side is

opaque. Figure 1 represents the mechanism of the sunlight absorption between monofacial PV and bifacial PV panel.

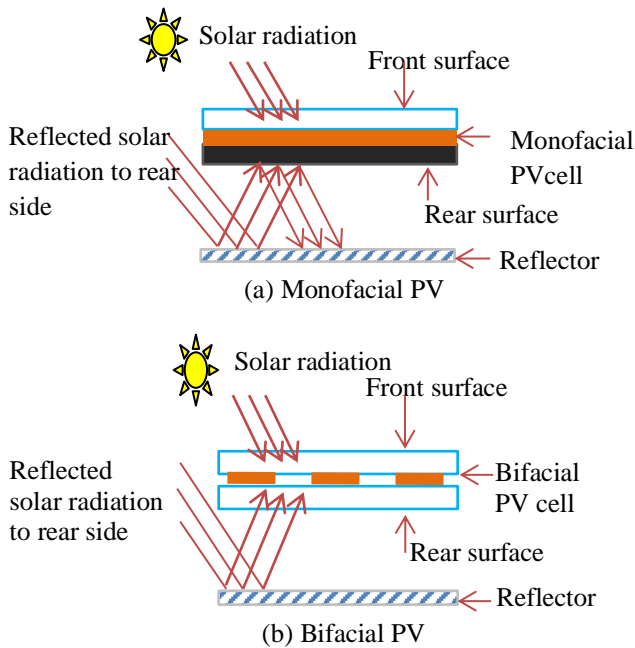


Fig. 1. Mechanism of sunlight absorption of (a) monofacial PV panel and (b) bifacial PV panel [16].

Additional electrical conversion efficiency of the bifacial PV panel is about 30% to 90% compared with conventional PV [17]. Ooshaksaraei et al. [18] described higher electricity generation of bifacial PV cells is due to the solar radiation absorption by the lower face of the panel. Yet another research by Yang et al. [19] determined that industrialized bifacial PV has 16.6% of front efficiency whereas 12.8% of rear efficiency. Lim et al [20] revealed that the total power production of bifacial PV with reflective mirror below the bottom surface of the panel is about 38.1%. Power generation of bifacial PV can be optimized by altering reflective materials

beneath the panel such as semi-mirror, mirror and diffuse. The electrical energy produced by the rear surface of bifacial PV strongly depends on types of reflector.

This paper introduces a new theoretical (mathematical modeling) of air-based BPVT collector with v-groove mirror reflector. In this study, BPVT collector was fabricated with double channel configuration. This study aims to develop a mathematical model to evaluate energy efficiency of BPVT. The influences of the mass flow rate, packing factor and solar radiation intensity on the collector performance were analyzed.

2. Mathematical Model

2.1. Energy Balance Equations

In this study, a new design of double-pass BPVT collector was developed. The BPVT collector is composed of glass cover, bifacial PV panel, V-groove reflector and insulator. Air flows through the first channel and then through the second channel of the collector. Figure 2 shows the heat transfer coefficients that are involved in bifacial PVT collector designed in this study. The following assumptions were made to develop energy balance equations:

- i. The heat transfer along the channels is forced convection.
- ii. Front and rear faces of the bifacial panel have the same values of electrical efficiencies.
- iii. The temperatures of both surfaces are assumed to be the same.
- iv. Heat absorption by air flows along the collector is uniform
- v. There are no thermal losses from the collector

According to Fig. 2, the energy balance equations at steady-state condition of the bifacial PVT collector can be written as shown in Table 1.

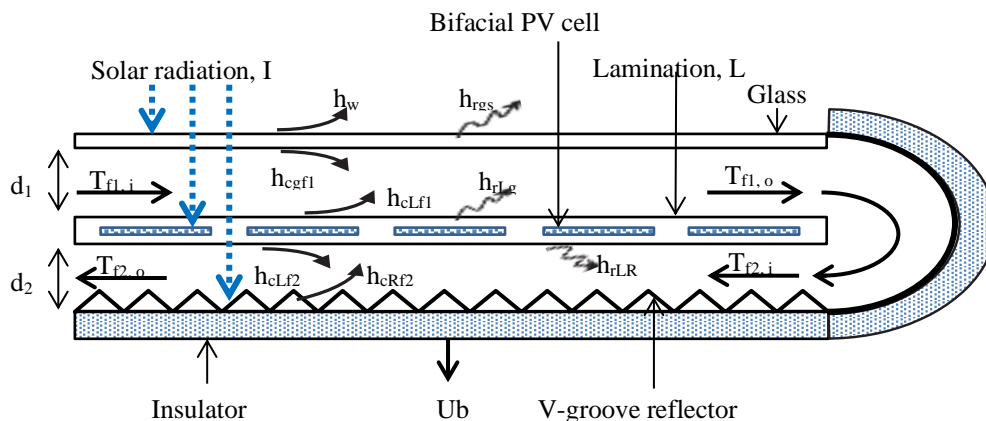


Fig. 2. Cross-sectional view of the heat transfer coefficients in a double-pass BPVT collector

Table 1. Energy balance equations

Energy Balance Equations	
i.	Glass cover $I_g + h_{rLg}(T_L - T_g) = U_t(T_g - T_a) + h_{cgf1}(T_g - T_{f1})$ (1)
ii.	Air flow in the upper channel $h_{cgf1}(T_g - T_{f1}) + h_{clf1}(T_L - T_{f1}) = (2mC/WL)T_i$ (2)
iii.	PV laminate $I_{pv} = h_{clf1}(T_L - T_{f1}) + h_{rLg}(T_L - T_g) + h_{clf2}(T_L - T_{f2}) - h_{rLR}(T_L - T_R)$ (3)
iv.	Air flow in the lower channel $h_{clf2}(T_L - T_{f2}) + h_{crf2}(T_R - T_{f2}) = 4mC/WL$ (4)
v.	Reflector $I_R + h_{rLR}(T_L - T_R) = h_{crf2}(T_R - T_{f2}) + U_r(T_R - T_a)$ (5)

The solar radiation captured by the glass cover per unit area is calculated by:

$$I_g = \alpha I \tag{6}$$

By considering the packing factors, P, of the bifacial PV panel, I_{pv} and I_R can be written as:

$$I_{pv} = I\tau_g\alpha_{pv}P(1 - \eta_{front}) + I\tau_g\tau_L\alpha_{pv}P(1 - P)\eta_R(1 - \eta_{rear}) \tag{7}$$

$$I_R = I(1 - P)\tau_L\tau_g(1 - \eta_R) \tag{8}$$

As stated by Eq. (7) and Eq. (8), most of irradiance is converted to electricity by the PV cells when the sunlight passes through the glazing and strikes to the bifacial panel. Then, some of irradiance is absorbed by PV lamination. Another remaining irradiance directly strikes to the reflector and it reflected back to the lower face of bifacial PV panel.

2.2. Heat Transfer Coefficients

The radiative and convective heat transfer coefficients of the collector are selected from the numerous number of literatures [21], [22].

$$h_w = 2.8 + 3.3v \tag{9}$$

where h_w is the convection heat transfer coefficient due to wind, and v is the air velocity over the glazing, $v = 1\text{ms}^{-1}$.

In this study, the radiative heat transfer coefficient from the glass cover to the sky is written by:

$$h_{rgs} = \frac{\sigma\epsilon_g(T_g + T_s)(T_g^2 + T_s^2)(T_g - T_s)}{T_g - T_a} \tag{10}$$

where sky temperature, T_s , is given by [23]:

$$T_s = 0.0552T_a^{1.5} \tag{11}$$

The radiative heat transfer coefficient between the glazing, PV laminate and reflector are stated by Eq. (12) and Eq. (13), respectively [24]:

$$h_{rLg} = \frac{\sigma(T_L + T_g)(T_L^2 + T_g^2)}{\frac{1}{\epsilon_L} + \frac{1}{\epsilon_g} - 1} \tag{12}$$

$$h_{rLR} = \frac{\sigma(T_L + T_R)(T_L^2 + T_R^2)}{\frac{1}{\epsilon_L} + \frac{1}{\epsilon_R} - 1} \tag{13}$$

The convective heat transfer coefficient due to airflow in the channels is determined by using following relations:

$$h_c = \frac{kNu}{D_h} \tag{14}$$

The hydraulic diameter for the v-groove reflector is equal to [25]:

$$D_h = \frac{2H_g \sin(\frac{\theta}{2})}{1 + \sin(\frac{\theta}{2})} \tag{15}$$

where θ is the angle of the v-groove reflector.

The Nusselt number, Nu for laminar, transition and turbulent flow region can be determined by [14], [21]:

i. $Re < 2300$ (16)

$$Nu = 5.4 + \frac{0.0019[RePr\frac{D_h}{L}]^{1.71}}{1 + 0.00563[RePr\frac{D_h}{L}]^{1.71}}$$

ii. $2300 < Re < 6000$ (17)

$$Nu = 0.116 \left[(Re^{\frac{2}{3}} - 125) Pr^{\frac{1}{3}} \right] \left[1 + \left(\frac{D_h}{L} \right)^{\frac{2}{3}} \right] \left[\frac{\mu^{0.14}}{\mu_w} \right]$$

iii. $Re > 6000$ (18)

$$Nu = 0.18Re^{0.8}Pr^{0.4}$$

where

$$\text{Prandtl, } Pr = \frac{\mu C}{k} \tag{19}$$

$$\text{Reynolds number, } Re = \frac{mD_h}{A\mu} \tag{20}$$

Finally, the physical properties of air are assumed to vary linearly with temperature (°C) as listed below [22]:

$$\text{i. Viscosity, } \mu = [1.983 + 0.00184(T - 27)] \times 10^{-5} \tag{21}$$

$$\text{ii. Specific heat, } C = [1.0057 + 0.000066(T - 300)] \tag{22}$$

$$\text{iii. Thermal conductivity, } k = 0.02624 + 0.0000758(T_p \times 300) \tag{23}$$

$$\text{iv. Density, } \rho = 1.1774 - 0.00359(T_p \times 300) \tag{24}$$

2.3. Simulation Procedures

The simulation procedure is described details in the flowchart as shown in Fig. 3. The geometrical, thermal and physical values listed in Table 2 were applied in the simulation. The equations listed above have been solved by using matrix inversion method. Eqs. (1)-(5) were presented in a 5x5 matrix form and simulated by Microsoft Excel software.

[A][T] = [C]

$$\begin{bmatrix} S_6 & S_7 & S_8 & 0 & 0 \\ S_9 & S_{10} & S_{11} & 0 & 0 \\ S_{12} & S_{13} & S_{14} & S_{15} & S_{16} \\ 0 & S_{17} & S_{18} & S_{19} & S_{20} \\ 0 & 0 & S_{21} & S_{22} & S_{23} \end{bmatrix} \begin{bmatrix} T_g \\ T_{f1} \\ T_L \\ T_{f2} \\ T_R \end{bmatrix} = \begin{bmatrix} S_1 \\ S_2 \\ S_3 \\ S_4 \\ S_5 \end{bmatrix}$$

where

- $S_1 = I_1 + U_t(T_a)$
- $S_2 = -(2mC/WL)T_i$
- $S_3 = I_2$
- $S_4 = -S_2$
- $S_5 = I_3 + U_R(T_a)$
- $S_6 = h_{cgf1} + h_{rLg} + U_t$
- $S_7 = -h_{cgf1}$
- $S_8 = -h_{rLg}$
- $S_9 = h_{cgf1}$
- $S_{10} = -(h_{cgf1} + h_{clf1})$
- $S_{11} = h_{clf1}$
- $S_{12} = -h_{rLg}$
- $S_{13} = -h_{clf1}$
- $S_{14} = h_{clf1} + h_{clf2} + h_{rLg} + h_{rLR}$
- $S_{15} = -h_{clf2}$
- $S_{16} = -h_{rLR}$
- $S_{17} = \frac{4mC}{WL}$
- $S_{18} = h_{clf2}$

$$S_{19} = -[h_{clf2} + h_{crf2} + \left(\frac{2mC}{WL}\right)]$$

$$S_{20} = h_{crf2}$$

$$S_{21} = h_{rLR}$$

$$S_{22} = h_{crf2}$$

$$S_{23} = -[h_{rLR} + h_{crf2} + U_R]$$

$$U_t = \left(\frac{1}{h_w + h_{rgs}}\right)^{-1}$$

$$U_b = \frac{k}{x}$$

where,

k = thermal conductivity of insulation

x = thickness of the rear insulation

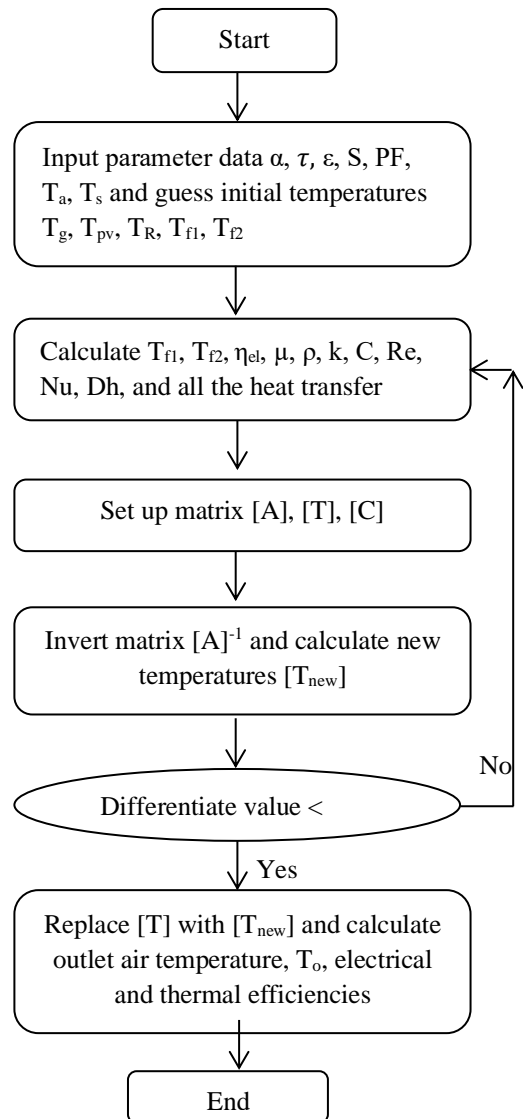


Fig. 3. Flowchart for the simulation program

Table 2. The geometrical, thermal and physical values used in the simulation

Parameters	Numerical values
Collector width, W	0.70 m
Collector length, L	0.70 m
Upper channel depth, d ₁	0.10 m
Lower channel depth, d ₂	0.10 m
Electrical efficiency at reference condition, η _{ref}	16 %
Temperature coefficient, β	0.0045 °C ⁻¹
Ambient temperature, T _a	25 °C
Inlet air temperature, T _i	25 °C
Mass flow rates, m	0.02kg/s,0.03 kg/s,0.04 kg/s,0.05kg/s, 0.06 kg/s
Solar radiation, I	667 Wm ⁻² , 863 Wm ⁻²
Packing factor, PF	0.33, 0.67
Transmittance of glass, τ _g	0.80
Transmittance of PV panel, τ _{PV}	0.04
Transmittance of lamination, τ _L	0.85
Absorption of glass, α _g	0.15
Absorption of PV panel, α _{PV}	0.91
Absorption of lamination, α _L	0.10
Absorption of reflector, α _r	0.3
Reflectance of glass, r _g	0.05
Reflectance of lamination, r _L	0.05
Reflectance of reflector, r _R	0.7
Emissivity of glass, ε _g	0.80
Emissivity of PV panel, ε _{PV}	0.6
Emissivity of reflector, ε _g	0.09

2.4. Energy Analysis

The following equations were used to determine the performances of the bifacial PVT collector. Both sides of

bifacial cells are involved in production of electricity, where the total electrical efficiency, η_{PV} was calculated by adding the electrical efficiency of front and rear surface.

$$\eta_{PV} = \eta_{PV_{front}} + \eta_{PV_{rear}} \tag{25}$$

Meanwhile, the electrical efficiency varies according to the temperature of the PV cell, T_{PV}, as below [26]:

$$\eta_{PV_{front}} = \eta_{PV_{rear}} = [\eta_{ref}(1 - \beta(T_{PV} - T_{ref}))] \tag{26}$$

where,

$$T_{ref} = 25^{\circ}C$$

η_{ref} = electrical efficiency at T_{ref} = 25°C

β = temperature coefficient at T_{ref} = 25°C

The thermal efficiency of PVT collector is considered as the total useful heat gain to incident solar radiation striking on the collector surface

$$\eta_{th} = \frac{mC(T_{out} - T_{in})}{A_c I} \tag{27}$$

where m, C, T_{out}, T_{in}, A_c and I are the mass flow rate, specific heat capacity of the fluid, outlet temperature, inlet temperature, area of collector and solar irradiance, respectively.

Thus, the total energy efficiency of PVT collector can be expressed by the sum of thermal and electrical energy efficiency, written as below:

$$\eta_{PVT} = \eta_{PV} + \eta_{th} \tag{28}$$

3. Result and Discussion

Table 3 displayed the theoretical results of the effects of solar radiation and packing factors on energy efficiency at various mass flow rates.

Table 3. Appearance properties of accepted manuscripts

m (kgs ⁻¹)	I (Wm ⁻²)	Packing factor, (PF)	T _{out} (°C)	T _{PV} (°C)	Efficiency (%)	
					Thermal	Electrical
0.02	667	0.33	30.91	57.52	24.09	5.14
		0.66	31.61	74.80	28.38	8.13
	863	0.33	32.15	66.52	24.49	4.93
		0.66	32.99	87.56	28.47	7.62
0.03	667	0.33	30.18	49.56	29.31	5.33
		0.66	31.01	63.07	37.00	8.61
	863	0.33	31.21	56.48	30.05	5.16
		0.66	32.25	73.30	37.48	8.19
0.04	667	0.33	29.60	45.21	32.03	5.43
		0.66	30.37	56.41	41.48	8.88
	863	0.33	30.47	50.88	32.99	5.30
		0.66	31.44	64.97	42.25	8.53
0.05	667	0.33	29.19	42.43	33.72	5.50
		0.66	29.88	52.07	44.24	9.06
	863	0.33	29.93	47.27	34.84	5.38
		0.66	30.80	59.49	45.21	8.76
0.06	667	0.33	28.89	40.48	34.89	5.54
		0.66	29.50	49.00	46.12	9.18
	863	0.33	29.53	44.73	36.13	5.44
		0.66	30.31	55.56	47.24	8.92

The performances of the BPVT collector have analyzed in terms of the output of the electrical and thermal energy. The energy of the BPVT collector influenced by mass flow rates, packing factors and solar radiation has been investigated. Changing the mass flow rates of working fluid influenced the output temperature and bifacial PV panel temperature as stated in Table 3. It can be noticed that when the mass flow rate keeps on increasing, the outlet temperature and temperature of PV panel will drop.

According to the simulation result, both electrical and thermal energy similarly to increase as the packing factor of bifacial PV panel increased. Regarding Figure 4 and 5, the electrical efficiency does not depend much on the mass flow rates compared with the thermal efficiency. As can be observed, increasing of thermal efficiency is about 20% at range of mass flow rate among 0.02 kg/s to 0.06 kg/s. The optimum thermal efficiency is 47% at mass flow rate of 0.06kg^s⁻¹ and solar radiation of 863Wm⁻².

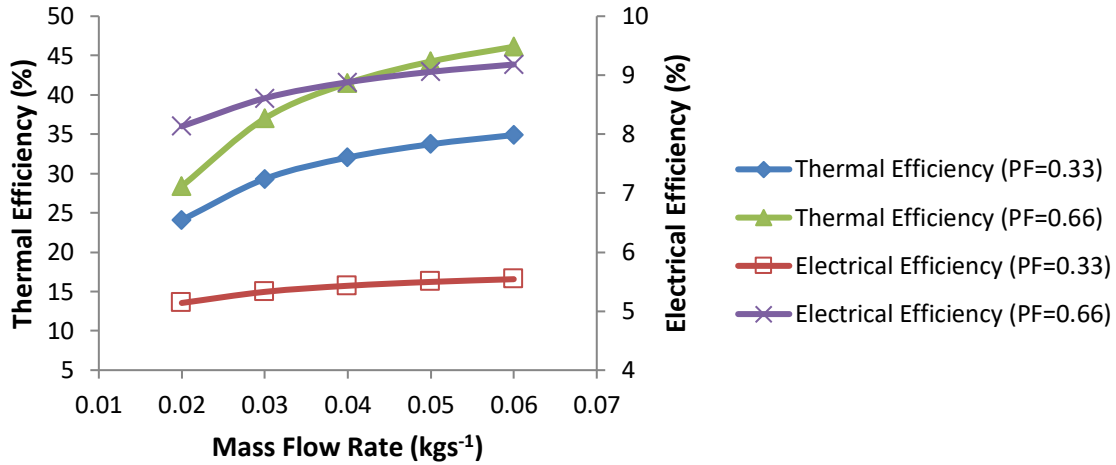


Fig. 4. Energy efficiency with variation in mass flow rates and packing factors at solar radiation of 667 Wm⁻²

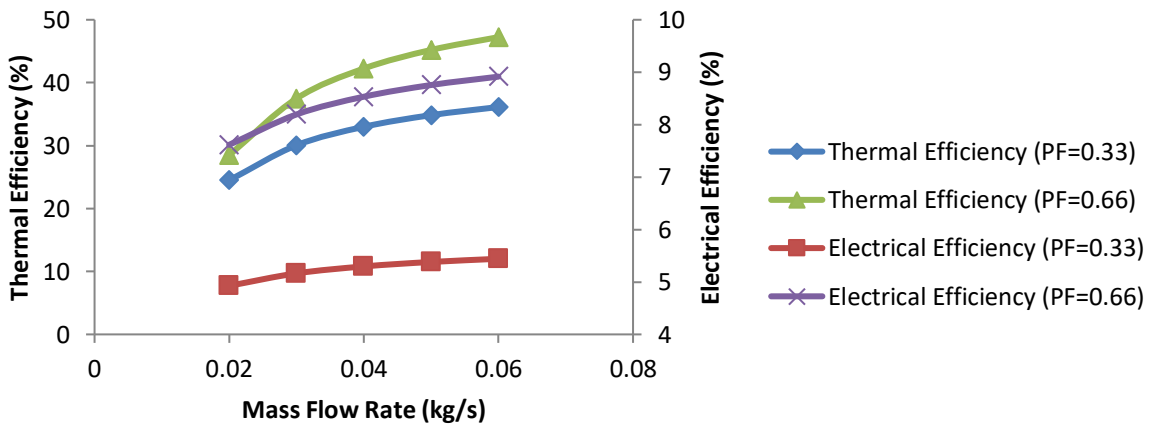


Fig. 5. Energy efficiency with variation in mass flow rates and packing factors at solar radiation of 863 Wm⁻²

At fixed solar intensity level, the electrical efficiency increased as the packing factor of the PV panel increases due to the larger amount of solar radiation absorption by bifacial PV cells. Both surfaces of the bifacial solar cells have the ability to absorb solar radiation, which is a promising in enhancing electricity generation [18]. Higher packing factor contributes to raising energy efficiency as shown in Fig. 5. BPVT collector has highest energy efficiency is about 57% at 0.66 of packing factor compared to the panel of 0.33 of packing factor which is 42%.

Figure 7 represented the comparison of energy efficiency of monofacial PVT collector and bifacial PVT collector which obtained from the simulation result. Bifacial PVT collectors produced higher energy efficiency compared to the one of similar monofacial PV panel design. Enhancement of energy efficiency is caused by higher internal forced convection heat transfer coefficient, lower PV panel operation temperature and consequently, the higher electrical efficiency of PV panel. Bifacial PVT collector has greater energy efficiency of 57% is than monofacial PVT collector, which has energy efficiency of 48% under the same parameters.

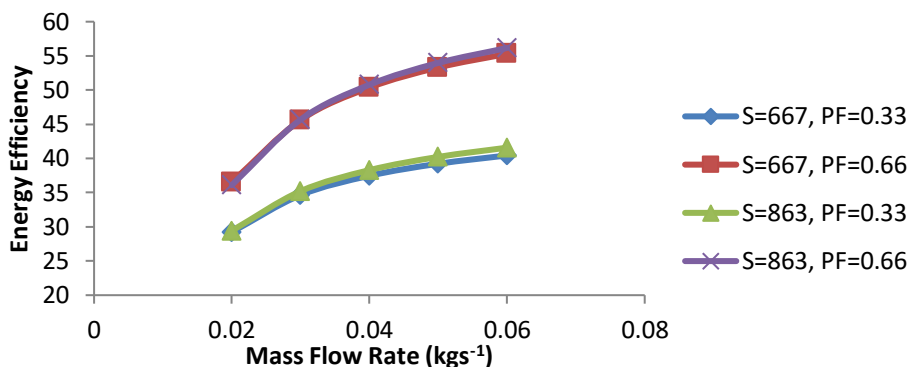


Fig. 6. Comparison of energy efficiency with variation in mass flow rates, packing factors and solar radiation

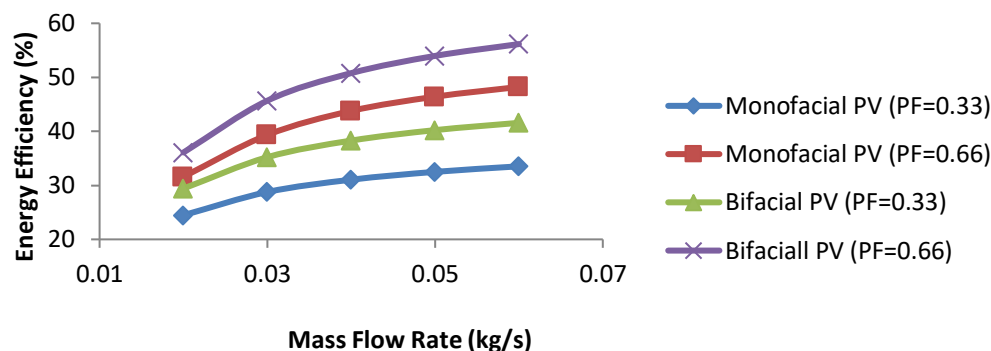


Fig. 7. Comparison of energy efficiency between monofacial PVT and bifacial PVT collector

The mathematical model of the BPVT collector developed in this research and its performances are validated using the experimental results that have been done by other researchers. The comparison indicates that the energy

efficiency of the present study was 20-57% that shows good agreement with previous system studied by Ooshaksaraei et. al [27] as shown in Table 4.

Table 4. Appearance properties of accepted manuscripts

Types of PVT collector	Energy Efficiency (%)	References
Water-based PVT collector in laminar and turbulent floc regime	87.0	[28]
PVT collector with dual channels for different fluid	76.2	[29]
Partially covered hybrid PVT flat plate collector solar still	85.0	[30]
Double pass PVT air collector	80.5	[31]
Uncovered and covered PVT water collector	35.4 – 43.6	[32]
Sheet-and-tube hybrid PVT water collector	55.0 – 80.0	[33]
PVT system using aluminium cooling plate with straight and helical channels	49.3 - 85	[13]
PVT air collector with ▽-groove	21.3-82.9	[14]
Air-based PVT collector with bifacial modules and semi-mirror reflector	28.0 – 67.0	[27]
Double-pass bifacial PVT collector with mirror reflector	20.0 – 57.0	Present study

4. Conclusion

This paper presented a mathematical model of BPVT collector with mirror reflector and procedure of simulation for performances analysis. The influences of the packing factor, mass flow rate and solar radiation on electrical and thermal efficiency were evaluated. The simulation analysis indicated that the improvement of energy efficiency is proportional to the increasing of packing factor, solar radiation and mass flow rate. The optimum energy efficiency of BPVT collector is approximately 57%, which was observed at the packing factor of 0.66 and mass flow rate is 0.06kgs-1

Acknowledgements

The authors would like to express their grateful acknowledgement to National University of Malaysia for funding GP-K020448.

References

- [1] M. Beken, B. Hangan and O. Eyecioglu, "Classification of Turkey among European Countries by Years in Terms of Energy Efficiency, Total Renewable Energy, Energy Consumption, Greenhouse Gas Emission and Energy Import Dependency by Using Machine Learning," *2019 8th International Conference on Renewable Energy Research and Applications (ICRERA)*, Brasov, Romania, 2019, pp. 951-956.
- [2] K. C. Wijesinghe, "Optimized Integration of Solar PV Energy on to Telecom Power Systems for DC and A/C buses or Energy Storages with proposed Converters to make them as profit centers," *2019 8th International Conference on Renewable Energy Research and Applications (ICRERA)*, Brasov, Romania, 2019, pp. 545-550.
- [3] A. Harrouz, M. Abbes, I. Colak and K. Kayisli, "Smart grid and renewable energy in Algeria," *2017 IEEE 6th International Conference on Renewable Energy Research and Applications (ICRERA)*, San Diego, CA, 2017, pp. 1166-1171.
- [4] M. E. Oruc, A. V Desai, P. J. A. Kenis, and R. G. Nuzzo, "Comprehensive energy analysis of a photovoltaic thermal water electrolyzer," *Appl. Energy*, vol. 164, pp. 294–302, 2016.
- [5] E. Skoplaki and J. A. Palyvos, "On the temperature dependence of photovoltaic module electrical performance: A review of efficiency / power correlations," *Sol. Energy*, vol. 83, no. 5, pp. 614–624, 2009.
- [6] M. N. Abu Bakar, M. Othman, M. Hj Din, N. A. Manaf, and H. Jarimi, "Design concept and mathematical model of a bi-fluid photovoltaic/thermal (PV/T) solar collector," *Renew. Energy*, vol. 67, pp. 153–164, 2014.
- [7] S. S. S. Baljit, H. Chan, and V. Adidharma , "Mathematical Modelling Of A Dual-Fluid Concentrating Photovoltaic-Thermal (PV-T) Solar Collector," *Renew. Energy*, vol. 114, pp. 1258–1271, 2017.
- [8] M. Mustapha, A. Fudholi, C. H. Yen, and M. H. Ruslan, "Review on Energy and Exergy Analysis of Air and Water Based Photovoltaic Thermal (PVT) Collector," *Int. J. Power Electron. Drive Syst.*, vol. 9, no. 3, pp. 1367–1373, 2018.
- [9] P. Gang, F. Huide, Z. Huijuan, and J. Jie, "Performance study and parametric analysis of a novel heat pipe PV / T system," *Energy*, vol. 37, no. 1, pp. 384–395, 2012.
- [10] A. Harrouz, I. Colak and K. Kayisli, "Energy Modeling Output of Wind System based on Wind Speed," *2019 8th International Conference on Renewable Energy Research and Applications (ICRERA)*, Brasov, Romania, 2019, pp. 63-68.
- [11] V. Msomi and O. Nemraoui, "Improvement of the performance of solar water heater based on nanotechnology," *2017 IEEE 6th International Conference on Renewable Energy Research and Applications (ICRERA)*, San Diego, CA, 2017, pp. 524-527.
- [12] M. J. M. Pathak, P. G. Sanders, and J. M. Pearce, "Optimizing limited solar roof access by exergy analysis of solar thermal, photovoltaic, and hybrid photovoltaic thermal systems," *Appl. Energy*, vol. 120, pp. 115–124, 2014.
- [13] M. R. Salem, R. K. Ali, and K. M. Elshazly, "Experimental investigation of the performance of a hybrid photovoltaic / thermal solar system using aluminium cooling plate with straight and helical channels," *Sol. Energy*, vol. 157, pp. 147–156, 2017.
- [14] A. Fudholi, M. Zohri, A. Ibrahim, C. H. Yen, M. Y. Othman, M. H. Ruslan and K. Sopian, "Energy and exergy analyses of photovoltaic thermal collector with ∇ -groove," *Sol. Energy*, vol. 159, pp. 742–750, 2018.
- [15] M. Yesilbudak, M. Colak, and R. Bayindir, "What are the current status and future prospects in solar irradiance and solar power forecasting?," *Int. J. Renew. Energy Res.*, vol. 8, no. 1, pp. 635–648, 2018.
- [16] A. Fudholi, M. Mustapha, I. Taslim, F. Aliyah, and A. G. Koto, "Photovoltaic thermal (PVT) air collector with monofacial and bifacial solar cells : a review," *Int. J. Power Electron. Drive Syst.*, vol. 10, no. 4, pp. 2021–2028, 2019.
- [17] K. M. T. Joge, Y. Eguchi, Y. Imazu, I. Araki, T. Uematsu, "Applications and field tests of bifacial solar modules," *Proc. 29th IEEE Photovolt. Spec. Conf.*, pp. 1549–1552, 2002.

- [18] P. Ooshaksaraei, K. Sopian, R. Zulkifli, M. A. Alghoul, and S. H. Zaidi, "Characterization of a Bifacial Photovoltaic Panel Integrated with External Diffuse and Semimirror Type Reflectors," *Int. J. Photoenergy*, vol. 2013, p. 7, 2013.
- [19] L. Yang, Q.H. Ye, A. Bong, W. T Song, G. J. Zhang, J. X. Wang and Y. Ma, "High efficiency screen printed bifacial solar cells on monocrystalline CZ silicon," *Prog. Photovoltaics Res. Appl.*, vol. 19, pp. 275–279, 2011.
- [20] Y. S. Lim, C. K. Lo, S. Y. Kee, H. T. Ewe, and A. R. Faiz, "Design and evaluation of passive concentrator and reflector systems for bifacial solar panel on a highly cloudy region: A case study in Malaysia," *Renew. Energy*, vol. 63, pp. 415–425, 2014.
- [21] N. S. Nazri, A. Fudholi, M. H. Ruslan, and K. Sopian, "Mathematical Modeling of Photovoltaic Thermal-Thermoelectric (PVT-TE) Air Collector," *Int. J. Power Electron. Drive Syst.*, vol. 9, no. 2, pp. 795–802, 2018.
- [22] A. Fudholi, M. Zohri, N. Shahirah, B. Rukman, and N. Syakirah, "Exergy and sustainability index of photovoltaic thermal (PVT) air collector: A theoretical and experimental study," *Renew. Sustain. Energy Rev.*, vol. 100, pp. 44–51, 2019.
- [23] W.C. Swinbank, "Long-wave radiation from clear skies," *J.R. Meteorol. Soc.*, vol. 89, pp. 339–348, 1963.
- [24] M. Zohri, L. D. Bakti, and A. Fudholi, "Exergy Assessment of Photovoltaic Thermal with V-groove Collector Using Theoretical study," *Telkomnika*, vol. 16, no. 2, pp. 550–557, 2018.
- [25] H. M. M. and F. A. A A Bashria, N M Adam, S M Sapuan, M Daud, H Omar, "Prediction of the thermal performance of solar air heaters by Internet-based mathematical simulation," *J. Power Energy*, vol. 218, pp. 579–587, 2004.
- [26] L. W. Florsschuetz, "Extension of the hottel-whillier model to the analysis of combined photovoltaic / thermal flat plate collectors," *Sol. Energy*, vol. 22, pp. 361–366, 1979.
- [27] P. Ooshaksaraei, K. Sopian, S. H. Zaidi, and R. Zulki, "Performance of four air-based photovoltaic thermal collectors configurations with bifacial solar cells," *Renewable Energy*, vol. 102, pp. 279–293, 2017.
- [28] F. Yazdanifard, E. Ebrahimmnia-Bajestan, and M. Ameri, "Investigating the performance of a water-based photovoltaic/thermal (PV/T) collector in laminar and turbulent flow regime," *Renew. Energy*, vol. 99, pp. 295–306, 2016.
- [29] D. Su, Y. Jia, X. Huang, G. Alva, Y. Tang, and G. Fang, "Dynamic performance analysis of photovoltaic – thermal solar collector with dual channels for different fluids," *Energy Convers. Manag.*, vol. 120, pp. 13–24, 2016.
- [30] D. B. Singh, J. K. Yadav, V. K. Dwivedi, S. Kumar, G. N. Tiwari, and I. M. Al-helal, "Experimental studies of active solar still integrated with two hybrid PVT collectors," *Sol. Energy*, vol. 130, pp. 207–223, 2016.
- [31] A. Slimani, M. Amirat, S. Bahria, I. Kurucz, and M. Aouli, "Study and modeling of energy performance of a hybrid photovoltaic / thermal solar collector: Configuration suitable for an indirect solar dryer," *Energy Convers. Manag.*, 2016.
- [32] N. Aste, C. Del Pero, and F. Leonforte, "Water PVT collectors performance comparison," *Energy Procedia*, vol. 105, pp. 961–966, 2017.
- [33] R. Liang, C. Zhou, Q. Pan, and J. Zhang, "Performance evaluation of sheet-and-tube hybrid photovoltaic / thermal (PVT) collectors connected in series," *Procedia Eng.*, vol. 205, no. 125, pp. 461–468, 2017.